HHS Public Access

Author manuscript

Addict Biol. Author manuscript; available in PMC 2018 November 01.

Published in final edited form as:

Addict Biol. 2017 November ; 22(6): 1743–1755. doi:10.1111/adb.12437.

Nicotine self-administration remodels perineuronal nets in ventral tegmental area and orbitofrontal cortex in adult male rats

Dolores B. Vazquez-Sanroman[1], **Reyna D. Monje**[2], and **M.T. Bardo**[1]

[1]Department of Psychology and Center for Drug Abuse Research Translation (CDART), University of Kentucky, Lexington KY, 40536, USA.

[2]Centro de Investigaciones Cerebrales (CICE), Universidad Veracruzana Unidad de Ciencias de la Salud Xalapa, Veracruz, 91010 México.

Abstract

Nicotine, a major psychoactive component of tobacco smoke, alters GABA modulation of dopamine (DA) neurons in the ventral tegmental area (VTA). Changes in structural neuroplasticity can occur in GABAergic parvalbumin (PRV) positive neurons, which are enveloped by structures of the extracellular matrix called perineuronal nets (PNNs). In the current study, rats were trained to self-administer IV nicotine (0.03 mg/kg/infusion) for 21 days in 1-h daily sessions with an incrementing fixed ratio requirement; a control group received saline infusions. At either 45 min or 72 hr after the last session, immunofluorescence measurements for PNNs, PRV and c-Fos were conducted. In VTA, nicotine self-administration reduced the number of PRV+ cells surrounded by PNNs at 45 min, as well as reducing the intensity of PNNs, suggesting a remodeling of GABA interneurons in this region; the number of PRV+ cells surrounded by PNNs was also reduced at 72 hr. A similar reduction of PNNs occurred in orbitofrontal cortex (OFC), but not in medial prefrontal cortex (PrL or IL), 45 min after the last session; PNNs were not detected in nucleus accumbens (shell or core). The reduction of PNNs in VTA and OFC was unrelated to c-Fos+ cells, as the percent of WFA+ cells co-expressing c-Fos was decreased in OFC, but not in VTA. Thus, nicotine self-administration remodeled PNNs surrounding GABA interneurons in VTA and its indirect connections to OFC, suggesting a new possible molecular target where nicotine-induced neuroplasticity takes place. PNN manipulations may prevent or reverse the different stages of tobacco addiction.

Keywords

c-Fos; nicotine self-administration; orbitofrontal cortex (OFC); perineuronal nets (PNNs); ventral tegmental area (VTA)

Corresponding author: Vazquez-Sanroman, Dolores B. Ph.D, Department of Psychology and Center for Drug Abuse Research Translation (CDART), University of Kentucky, Lexington KY, 40536 USA. dva226@uky.edu.

The authors declare no conflict of interest.

INTRODUCTION

Nicotine is the principle neuroactive component in tobacco that increases dopamine (DA) levels in the mesoaccumbens reward system (Di Chiara and Imperato, 1988). Midbrain DA cell bodies in the ventral tegmental area (VTA) subserve nicotine reward (Laviolette and van der Kooy, 2003). Within the VTA exists a population of GABA interneurons that provide inhibitory input to those DA neurons (Olson and Nestler, 2007). Nicotine excites GABA neurons and enhances GABAergic transmission transiently (Alkondon et al., 2000). Nicotine not only affects the activity of DA neurons through its actions on the inhibitory GABA neurons (Erhardt et al., 2002), but it also enhances glutamatergic transmission, with the net effect being a shift toward excitation of the DA reward system (Clemens et al., 2014). However, little is known about the morphological and structural changes induced in the VTA after nicotine self-administration. While one study has shown that nicotine self-administration has no effect on the size of DA soma in VTA (Mazei-Robison et al., 2014), that study did not examine GABAergic input processes.

Structural plasticity can be achieved through alterations of the extracellular matrix and perineuronal nets (PNNs) (Caroni et al., 2012). PNNs are net-like structures in the brain surrounding primarily GABAergic neuronal somas, dendrites and some synapses (Hartig et al., 1992). In the adult brain, remodeling of PNNs is directly linked to fast-spiking GABA neurons in several brain areas and may play a pivotal role in inhibiting drug-related behavior (Carulli et al., 2006; Vazquez-Sanroman et al., 2015). Functionally, PNNs may serve to maintain established neuronal connections (Murakami et al., 1999), as well as modulating impulse-regulating neurotransmitter release and growth factor supply (Carulli et al., 2013), and it has been suggested that these structures support the high firing frequencies of fast-spiking GABA interneurons (Van den Oever et al., 2010). Because of the critical function of PNNs in synaptic plasticity, disruption of these structures has been related to the neuronal circuitry dysfunction associated with drug addiction (Brown et al., 2008; Van den Oever et al., 2010).

One candidate thought to be involved in controlling PNN constitution within VTA is a family of endopeptidases called matrix metalloproteinases (MMPs) (Natarajan et al., 2013). Nicotine increases MMP9 expression and appears to be necessary for facilitating structural changes associated with acquisition of nicotine-induced conditioned place preference (Natarajan et al., 2013). PNNs can be recognized by the plant lectin Wisteria Floribunda agglutinin (WFA), a recognized marker for changes in the nets (Hartig et al., 1992). PNN remodeling seems to be specific for different brain regions and different types of memories (Gogolla et al., 2009). Although several studies have demonstrated a relationship between disruptions in PNNs and facilitation of drug memories (Slaker et al., 2015; Xue et al., 2014), it is not known if nicotine induces changes in PNNs in VTA or associated corticolimbic projections.

The purpose of the current study was to determine if acquisition of nicotine self-administration induces a remodeling of PNNs in PRV+ interneurons in VTA and OFC, which are critical nicotine reward brain regions. PNNs and c-Fos were measured either 45 min or 72 hr after the last self-administration session. For this study, VTA and NAc (core

and shell subregions) were examined due their role in nicotine reward and reinstatement (Corrigall et al., 1994; Gipson et al., 2013). Prelimbic cortex (PrL), infralimbic cortex (IL) and orbitofrontal cortex (OFC) were examined due to their role in impulsivity and addictive disorders (Perry et al., 2011)

METHODS

Animals

Thirty-eight adult male Sprague-Dawley rats (200-225 g body weight) were obtained from Harlan Industries (Indianapolis, IN, USA) and were single housed on a 12/12 hr light/dark cycle with ad libitum access to food and water in the home cage, except as noted below. All experiments were conducted during the light phase. Animals were housed and handled one week prior to the beginning of the experiments. All surgical and testing procedures were approved by the University of Kentucky Institutional Animal Care and Use Committee and conformed to NIH guidelines.

Apparatus

Nicotine self-administration was assessed in a standard two-lever operant conditioning chamber (ENV-001, Med Associates, St Albans, VT., USA). Two response levers were located on either side of a recessed food tray. Located above each lever was a white cue light. Nicotine or saline infusions were delivered by a syringe pump (Med Associates, PHM-100). A computer, linked to a Med Associates interface, recorded responses and controlled infusions during the experimental session.

Surgery

Animals were anesthetized and implanted with an intravenous jugular catheter as described previously (Green et al., 2000). Rats were allowed to recover for 1 week before starting nicotine self-administration. Daily infusions of heparinized saline were given to maintain patency of the catheters throughout the experiment.

Nicotine self-administration

To establish reliable nicotine self-administration, the general methods described previously were used (Corrigall and Coen, 1989). Prior to surgery, rats were food restricted to 85% of free-feed body weight and trained (9 days total) to press a lever for food reward (45 mg pellet, F0021, Bio-Serv, Flemington NJ). The schedule of food reinforcement during 60-min sessions was increased from a fixed ratio 1 (FR1), to a FR2, to a terminal FR5 schedule of reinforcement, with each FR requirement lasting 3 days. Subjects were then allowed ad libitum access to food and water for 48 hr, followed by surgical implantation of the catheter.

Nicotine self-administration was assessed during 60-min daily sessions. Nicotine (0.03 mg/kg per infusion) was infused (0.1 ml, 2.5 sec) immediately after meeting the schedule requirement on the active lever. The active lever for nicotine self-administration was the same lever used for food training. A 20-sec time-out period, concurrent with the beginning of the infusion, was signaled by illumination of both cue lights; responding on the inactive lever had no programmed consequence. Across sessions, the schedule of reinforcement was

increased from an FR1 (5 sessions), to an FR2 (3 sessions), to a terminal FR5 (13 sessions). Nicotine self-administration training continued until stable responding was obtained; stable responding was defined as less than 20% variability in infusions for the group across 3 consecutive sessions, with a minimum of 8 infusions per session and at least a 2:1 ratio of active:inactive lever responding. During the nicotine self-administration phase, food access was restricted to 20 g per day. A group of control rats was treated identically, except that saline was used instead of nicotine.

Perfusion and brain sampling

Following completion of nicotine self-administration, rats were deeply anesthetized with ketamine/xylazine cocktail and perfused transcardially with cold saline solution (0.9% NaCl) followed by cold 4% paraformaldehyde. After perfusion, brains were extracted and placed in 4% paraformaldehyde solution overnight, followed by 30% sucrose solution for 48-72 hr or until immersion. Using a frozen medium (Histoprep, Fisher scientific), brains were then immersed under liquid nitrogen for 20 sec. Consecutive coronal sections at 40 μm were obtained using a cryostat (Ag Protect Leyca CM 1860) and stored in a freezing solution (30% ethylene glycol, 25% glycerol, 30% sucrose in PBS) at −20°C.

Immunofluorescence

Free-floating sections were rinsed seven times for 15 min each with Triton X-100:1x tris-PBS (TPBS; Tris–HCl 10 mM, sodium phosphate buffer 10 mM, 0.9% NaCl, pH 7.4), and incubated with the following primary antibodies: (1) rabbit polyclonal anti-c-Fos antibody (sc-7202, Santa Cruz Biotechnology, CA, USA), diluted 1:200; (2) WFA (L1516-2MG, Sigma Aldrich, USA), diluted 1:200; (3) mouse monoclonal anti-PRV antibody (235, Swan, Swiss antibodies, Switzerland), diluted 1:1000; or (4) goat polyclonal anti-pDARPP-32 (sc-2161, Santa Cruz Biotechnology, CA, USA), diluted 1:200. Incubations were at 4°C for 48 hr in TPBS 0.1M Triton X-100 containing 3% of donkey serum. After rinsing, tissue was incubated for 2 hr at room temperature protected from light with one of the following secondary antibodies with conjugated fluorochromes: (1) Alexa Fluor 488 donkey anti-rabbit (A-21206, Life Technologies, USA), diluted 1:500; (2) Alexa Fluor 647 donkey anti-mouse (715-605-150, Jackson Labs, USA), diluted 1:500; or (3) biotinylated goat anti-rabbit conjugate with streptavidin Texas red (Vector Labs, UK), diluted 1:500. Once the fluorescence reaction occurred, sections were mounted using Mowiol 4-88 reagent (475904-100GM, EMD Millipore, USA).

Neuronal counting

Three fluorescent-labelled sections for each brain area (PrL, IL, OFC, NAc shell and core, and VTA; see Fig. 1) were examined using a confocal microscope (Nikon Eclipse-1C) by an observer who was not aware of the treatment condition for each section. Confocal images were taken in single XY planes, 1 μm thick, at a resolution of 1024 × 1024 and 100 Hz speed. Laser intensity, gain and offset were maintained constant in each analysis. Image analysis were made using the Image J software (NIH). In each brain area, 3 selected slices for c-Fos-IR, PRV-IR, and pDARPP-32-IR were estimated in a region of interest (ROI) of 40,000 μm^2. For c-Fos-IR, we considered a cell positive if it showed full nuclear and intense labelling. For quantification of PNNs, we estimated on double labeled sections the number

of PRV+ cells bearing PNNs by WFA. In each brain region, we sampled all the PRV+ interneurons within each ROI and assessed the presence of a PNN surrounding each individual neuron. Analysis of WFA staining intensity was performed on confocal images collected under a 40x objective with a 2.0 digital zoom. We measured the brightness intensity (range 0-255) of at least 50 PNNs/animal (n=6/experimental condition). We then randomly selected 15 points of densitometry covering the PNN area. The background brightness, taken from a non-stained region of the cortical molecular layer, was subtracted from each brightness measurement. Each net was assigned automatically to one of three categories of staining intensity, ranging from the lowest to the highest value of WFA intensity: faint 0-33%, medium 34-66% and strong 67-100% of maximum intensity. Nets touching the edges of the image were excluded. The densitometry analysis of the nets was performed in the soma area only (dendrites were not included) (Foscarin et al., 2011; Vazquez-Sanroman et al., 2015). Immunofluorescence results are represented as the average of densitometry and cell counts collected from the 3 brain slices selected.

Drugs

S(–)-Nicotine ditartrate was purchased from Research Biochemicals Inc. (Natick, Mass., USA). Nicotine was dissolved in sterile 0.9% NaCl (saline) and the pH was adjusted to 7.4 prior to injection. For surgical anesthesia, we used a mix of ketamine 31.25 mg/kg, xylazine HCl 6.25 mg/kg (Ana Sed, Lloyd Inc) and acepromazine maleate 1.25 mg/kg (Aceproject).

Statistics

All statistical analyses were conducted using STATISTICA 7 (Statsoft, Inc., Tulsa, OK, USA). Data were expressed as mean and standard error of the mean (SEM), and were analyzed using either parametric or non-parametric statistics. For parametric statistics, ANOVA was used, followed by *post-hoc* Tukey HSD tests. For nonparametric statistics, Chi-square tests were used to compare the distribution of frequencies relative to staining intensity categories of WFA+ cells. In all cases, the level of significance was set at $p< 0.05$. Total cellular expression of c-Fos was converted to mm^2.

RESULTS

Nicotine self-administration

Among the 38 rats that began the study, 6 were excluded from the analyses due to either loss of catheter patency or failure to meet the criteria to reach stable responding for nicotine during acquisition. The final group size for nicotine self-administration was N=17 and for saline control was N=15. At stable criteria, nicotine self-administration rats responded with an average (mean ± SEM) of 58.4 ± 5.3 active lever presses (11.6 ± 1.3 infusions) and saline control rats responded with 34.2 + 4.16 active lever presses (6.3 ± 1.6 infusions) during the 60-min session. Responding on the inactive lever was low (<15 responses per session) and there was no significant difference between nicotine and saline self-administration groups in inactive responding. A 2 × 2 × 21 (lever × drug × session) mixed factor ANOVA revealed main effects of lever ($F_{1,62}$=188.96 $p< 0.05$), drug ($F_{1,62}$=187.57 $p< 0.05$) and session ($F_{20,1240=}$23.11 $p< 0.01$), as well as a significant lever × drug × session interaction ($F_{20,1240}$=5.78 $p< 0.001$; Fig 2A). Across all sessions, both nicotine and saline rats

responded significantly more on the active lever than the inactive lever. More important, across incrementing FR sessions, nicotine self-administration rats showed an increase in responding on the active lever, whereas saline control rats did not; neither group showed a significant change in inactive lever pressing across sessions. When plotted as number of infusions across the FR5 sessions, a 2 × 13 repeated measures ANOVA revealed a main effect of drug ($F_{1,62=11.14}$ $p< 0.01$), with nicotine rats earning more infusions across all sessions compared to saline control (Tukey HSD $p<0.05$ from the 3rd to the 13th session in a FR5 schedule; Fig 2B). Finally, when plotted as total nicotine intake, there was no significant change in intake across the final 5 sessions (see Fig 2C for individual intake amounts in nicotine self-administration rats).

Cellular Immunofluorescence

VTA and NAc—In VTA, the majority (85-95%) of PRV+ cells also co-expressed WFA in saline controls (Fig 3A and B). Further, among those cells expressing WFA, 97% also expressed PRV (results not shown), indicating that PNNs in VTA were associated almost exclusively with GABAergic neurons. Nicotine self-administration decreased the percentage of PRV+ cells co-expressing WFA measured both 45 min ($F_{1, 15}$=8.20, $p<0.01$; Fig 3A) and 72 hr ($F_{1, 15}$=7.33, $p<0.01$; Fig 3B) after the last session; however, the total number of WFA + cells was not altered. Among those cells expressing WFA immunoreactivity, nicotine self-administration also induced a significant remodeling of PNNs in VTA after the last session, as reflected by a greater proportion of “faint” intensity compared to “strong” intensity WFA fluorescence 45 min after the last session (X^2 (1) =5.32, $p<0.05$; Fig 3C and Panel I). This nicotine-induced weakening in WFA intensity was transient, however, as it was not observed 72 hr after the last session (Fig 3D).

Regarding the effect of nicotine on c-Fos immunoreactivity, the total number of c-Fos+ cells was increased in VTA at 45 min ($F_{1, 15}$=48.23, $p<0.001$; Fig 3E and Panel J), but not at 72 hr after the last session (Fig 3F). However, there was no significant change in the percent of WFA+ cells co-expressing c-Fos (Figs 3G and H, and Panel J).

In both NAc shell and core, WFA immunoreactivity localized to cell bodies was essentially non-existent (results not shown); however, both pDARRP-32 and c-Fos immunoreactivity were analyzed in these regions. Figure 4 illustrates the results obtained from NAc shell. A one-way ANOVA revealed that nicotine self-administration did not modify the total number of pDARPP-32+ cells in NAc shell (Figs 4A and B, and Panel G). However, at 45 min after the last session, a one-way ANOVA revealed an increase in c-Fos expression in NAc shell ($F_{1, 15}$=4.94, $p<0.001$; Fig 4C and Panel G). Conversely, there was a significant decrease in c-Fos expression in NAc shell at 72 hr ($F_{1, 15}$=12.59, $p<0.001$; Fig 4D and Panel H). Further, nicotine increased the percentage of pDARPP-32+ cells in NAc shell that also co-expressed c-Fos at the 72 hr time interval ($F_{1, 15}$=16.32, $p<0.001$; Fig 4F and Panel H), but not at the 45 min time interval (Fig 4E and Panel G).

The results from NAc core are summarized in Table 1. As observed in NAc shell, nicotine self-administration did not modify the total number of pDARPP-32+ cells at either 45 min or 72 hr after the last session. In addition, similar to NAc shell, there was a significant increase in c-Fos expression at 45 min ($F_{1, 15}$=5.03, $p<0.05$); however, there was no significant effect

observed at 72 hr. There was no significant effect of nicotine self-administration on the percentage of pDARPP-32+ cells co-expressing c-Fos in NAc core.

PrL, IL and OFC—In saline controls, the majority (>60%) of PRV+ cells also co-expressed WFA in PrL and IL (Table 1), as well as in OFC (Fig 5A and B). Further, among those cells expressing WFA, >90% also expressed PRV (results not shown) in PrL, IL and OFC, indicating that PNNs in these prefrontal cortical regions were associated almost exclusively with GABAergic neurons. Regarding the effects of nicotine self-administration, there were no significant nicotine-induced changes in the number of WFA cells, c-Fos cells or PRV+ neurons at either 45 min or 72 hr after the last session in either PrL or IL (Table 1). In contrast, in OFC, there was a nicotine-induced decrease in the percentage of PRV+ neurons co-expressing WFA at 45 min ($F_{1, 15}$=17.08, p<0.001; Fig 5A), but not at 72 hr after the last session (Fig 5B). There was also a nicotine-induced increase in the "faint" intensity expression of WFA at 45 min (X^2 (1) =9.32, p<0.05; Fig 5C and Panel I), but not 72 hr after the last session (Fig 5D and Panel J), indicating a transient reduction in PNN intensity in OFC.

Analysis of c-Fos+ cells in OFC revealed a time-dependent change in immunoreactivity, with nicotine producing a decrease at 45 min ($F_{1, 15}$=6.13, p<0.05; Fig 4E and Panel I) and an increase at 72 hr after the last session ($F_{1, 15}$=9.56, p<0.05; Fig 4F and Panel J). There was also a nicotine-induced decrease in the percentage of WFA+ cells co-expressing c-Fos at the 45 min time interval ($F_{1, 15}$=12.03, p<0.01; Fig 5G Panel I), but not at the 72 hr time interval (Fig 5H and Panel J).

DISCUSSION

In the present study, we examined the effects of nicotine self-administration on PNNs, as well as on changes in c-Fos immunoreactivity, within VTA and its associated mesocortical projection sites. As expected, the behavioral results showed rates of nicotine self-administration that were stable and reliably greater than saline control by the end of training. In VTA, we found a nicotine-induced decrease in the percent of GABA neurons surrounded by PNNs at both 45 min and 72 hr after the last session. Further, there was reduced intensity of WFA+ fluorescence of PNNs at 45 min, but not after 72 hr. The reduced intensity of the PNNs was not related directly to c-Fos immunoreactivity. That is, while c-Fos+ cells in VTA were enhanced dramatically 45 min after the last session, there was no change in the percent of WFA+ cells co-expressing c-Fos, suggesting that the nicotine-induced increase in c-Fos expression was primarily associated with non-GABAergic neurons. However, since nicotine self-administration decreased the number of PRV+ cells co-expressing WFA, we cannot rule out the possibility that nicotine increased c-Fos expression in GABAergic neurons lacking PNNs. In any case, we can conclude that nicotine self-administration produced a transient reduction in the intensity of PNNs associated with PRV+ cells, suggestive of enhanced remodeling of intra-VTA GABAergic neurons.

To the best to our knowledge, this is the first study to demonstrate a nicotine-induced effect on PNN intensity within the VTA. Regardless of the exact mechanism involved, the reduced intensity expression of PNNs associated with VTA GABAergic neurons observed in the

current study is an important finding because both GABA and glutamate inputs into VTA modulate DA impulse flow, with a shift toward reduced GABA tone relative to glutamate tone following repeated nicotine treatment (Mansvelder and McGehee, 2002; Subramaniyan and Dani, 2015). Although we did not determine what functional consequences, if any, the decrease in PNN intensity had on VTA GABAergic neurons in the current study, previous electrophysiological evidence suggests that nicotine-induced remodeling of GABAergic interneurons may lead to enhanced burst firing of VTA DA neurons (Mansvelder and McGehee, 2002; Tolu et al., 2013), as well as perhaps altering the sensitivity of long-projecting VTA GABAergic neurons that innervate NAc shell and prefrontal cortex (Tolu et al., 2013). These cellular events may lead to a sensitized response to nicotine within VTA, thus playing a crucial role in the process of nicotine self-administration and addiction.

Similar to VTA, changes in PNN intensity were noted in OFC following nicotine self-administration. The OFC has connections with the mesolimbic DA system that is critical for drug reward (McFarland and Kalivas, 2001). Previous work has shown that OFC plays a critical role in modulating VTA dopaminergic activity related to expectancy of reward (Takahashi et al., 2011). Moreover, regarding the effects of nicotine specifically, acute intra-OFC nicotine stimulates GABAergic activity in this region (Cloke and Winters, 2015), while repeated systemic nicotine induces long-term epigenetic changes in OFC (Mychasiuk et al., 2013). The current results extend these results by showing that, similar to VTA, nicotine self-administration reduced the percentage of PRV+ cells co-expressing WFA. However, in contrast to VTA, this effect was only evident at the 45 min time interval, suggesting that the nicotine-induced changes in the intensity of PNNs on GABAergic interneurons is reversed more rapidly in OFC than VTA.

The pattern of c-Fos expression also differed between VTA and OFC. As mentioned previously, nicotine self-administration elevated c-Fos expression at 45 min, but not at 72 hr after the last session in VTA; however, this transient elevation was not associated with WFA + cells. In contrast, in OFC, nicotine self-administration first decreased c-Fos expression at 45 min, but then increased c-Fos expression at 72 hr. The rebound increase in c-Fos immunoreactivity noted at 72 hr may reflect a withdrawal effect. Although signs of withdrawal are typically associated with higher nicotine doses and more prolonged daily exposures than used here, at least one study has shown that acute nicotine (0.5 mg/kg) can produce spontaneous withdrawal (measured by intracranial self-stimulation thresholds) up to 74 hr after injection (Harris et al., 2013). Also contrasting with the results obtained in VTA, nicotine self-administration decreased the percent of PNNs co-expressing c-Fos in OFC, suggesting that nicotine altered the physiological properties of fast-spiking GABA interneurons within this area. While the mechanism by which PNN intensity in OFC is decreased by nicotine remains unknown, recent work has shown that i.c.v. injection of FN439, a broad spectrum MMP inhibitor, blocked the acquisition of nicotine conditioned place preference (Natarajan et al., 2013). Combined with our results in both VTA and OFC, it appears that digestive processes which reduce PNN intensity may be triggered by nicotine self-administration. Interesting, a similar conclusion has been made regarding the role of MMPs in altering synaptic remodeling in the medial prefrontal cortex related to formation of memories underlying cocaine reinstatement (Brown et al., 2008).

In contrast to both VTA and OFC, nicotine self-administration had no effect on any measure of PRV, WFA or c-Fos immunoreactivity in PrL or IL. This was surprising since GABAergic receptors in PrL and IL have been strongly implicated in reinstatement of nicotine seeking (Lubbers et al., 2014). However, since we did not assess reinstatement in the current study, it is possible that significant cellular effects would have been obtained if nicotine seeking was reinstated after a period of extinction or abstinence. Contrary to our negative results with c-Fos immunoreactivity in PrL and IL, a previous study found that nicotine self-administration increased c-Fos immunoreactivity in medial prefrontal cortex (Pagliusi et al., 1996). These discrepant results are not likely due to differences in nicotine self-administration parameters or dose, as both studies used the same well-established behavioral procedure (Corrigall and Coen, 1989). More likely, a difference in antibodies used may explain the discrepant findings. Specifically, the previous study used a general antibody that recognizes a c-Fos fraction, but also Fos-related antigens (c-Fos, FosB, FRA1), whereas our study used a more specific c-Fos antibody. In any case, the varied pattern of c-Fos results obtained within PrL, IL, and OFC indicates that more work is needed to shed light on the region-specific differences in neuronal activity within these cortical regions following nicotine.

There was no evidence of WFA+ cells in NAc shell or core, which is consistent with previous results (Hartig et al., 1992). However, as expected, nicotine self-administration increased c-Fos expression in NAc (shell and core) 45 min after the last session. In agreement with this, previous studies have shown that nicotine self-administration increases c-Fos immunoreactivity 30 min after the last session in each of these reward-relevant brain regions (Clemens et al., 2014). There was also a rebound decrease in c-Fos activity obtained in NAc shell at 72 hr in the current study. Additional cellular analysis in NAc shell revealed that the percent of dopaminoceptive pDARRP-32+ cells expressing c-Fos was decreased, suggesting a reduction of DA tone in this terminal field 72 hr after the last session, which is likely associated with the anhedonia that occurs at this time point (Harris et al., 2013; Stoker et al., 2012)

One limitation of this study is that a short-access (60 min daily) schedule of nicotine self-administration was used, which may have been less than optimal for modeling human tobacco dependence. In contrast to short-access schedules, long-access (23 hr) self-administration sessions can achieve levels of nicotine found in human smokers (Sanchez et al., 2014). However, nicotine is not the only tobacco constituent involved in addiction. For example, the tobacco alkaloid and active nicotine metabolite nornicotine serves as a both a psychostimulant and positive reinforcer in rats (Bardo et al., 1999; Green et al., 2001). Nornicotine has an 8X longer plasma half-life compared to nicotine in both human smokers and non-smokers (Kyerematen et al., 1994), and is known to accumulate in rat brain with repeated intermittent peripheral injections (Ghosheh et al., 1999). Thus, even the short-access schedule used here would be expected to provide an extended post-session period of nicotinic receptor activation, which is a critical component for the addictive process.

Another potential limitation of the self-administration procedure used is the possible effects of food pretraining and/or food restriction during nicotine sessions on PNN intensity in VTA and OFC. We selected this procedure to conform to previous work from our laboratory and others (Corrigall et al., 1994; Green et al., 2000). Food pretraining allows for high rates of

responding during the first self-administration session, thus promoting rapid acquisition. Due to this food pretraining, it could be argued that substituting saline for food reward produced greater extinction learning than substituting nicotine for food reward, thus leading to the cellular effects observed. While we cannot dismiss this possibility completely, it is notable that while the nicotine group showed less responding than the saline group across the initial five FR1 sessions (due to the response suppressant effects of nicotine), both groups showed a similar decrease in responding (extinction) across these initial sessions. Moreover, the performance of saline rats across the FR2 and FR5 sessions showed no decrement in lever pressing, which is inconsistent with an extinction interpretation.

A third potential limitation in the behavioral procedures relates the use of the saline control group. There are a several other control groups that could have been incorporated into our experimental design such as a non-contingent yoked control or naïve non-extinguished control. However, a problem with both a yoked saline and naïve control group is that neither would have controlled for differences in the reinforcing effect of the cue light illumination that signaled each nicotine or saline infusion. As shown previously, rats will lever press simply for contingent cue light illumination and this responding is enhanced by nicotine (Chaudhri et al., 2007). Indeed, the reinforcing effect of cue light illumination likely explains the sustained rate of active lever pressing in saline controls in the current study, as well as perhaps the secondary reinforcing effect of cue light illumination due its previous association with food. In any case, in contrast to either a yoked saline or naïve group, the current saline group controlled for potential cellular changes induced by response-contingent cue light illumination.

In summary, these results corroborate evidence indicating that nicotine increases c-Fos expression in regions associated the processing of nicotine reward, including NAc core and shell, VTA and OFC. More important, the current study extends these results by showing that nicotine self-administration reduces PNN intensity associated with GABA neurons in VTA, as well as in OFC, which may play a critical role in remodeling of neurocircuits underlying nicotine addiction. Reduced intensity of PNNs within VTA and OFC may be associated with reduced inhibitory function of GABAergic interneurons, thus promoting sensitization of DA burst firing in VTA and leading to acquisition of nicotine self-administration and addiction. Since both VTA and OFC are structures involved with compulsive behaviors (Volkow and Fowler, 2000), manipulation of PNNs during nicotine self-administration might offer a novel approach for understanding the mechanisms of nicotine reward, thus offering a potential new approach for treating tobacco dependence.

ACKNOWLEDGEMENTS

This work was supported by: NIH grants P50 DA05312 and R01 DA12964

We thank Emily Denehy and Seth Mayfield for technical support. We thank Drs. Mark Prendergast and James Pauly for allowing us the use of equipment.

1. REFERENCES

2. Alkondon M, Braga MF, Pereira EF, Maelicke A, Albuquerque EX. alpha7 nicotinic acetylcholine receptors and modulation of gabaergic synaptic transmission in the hippocampus. Eur J Pharmacol. 2000; 393:59–67. [PubMed: 10770998]
3. Bardo MT, Green TA, Crooks PA, Dwoskin LP. Nornicotine is self-administered intravenously by rats. Psychopharmacology (Berl). 1999; 146:290–296. [PubMed: 10541729]
4. Brown TE, Forquer MR, Harding JW, Wright JW, Sorg BA. Increase in matrix metalloproteinase-9 levels in the rat medial prefrontal cortex after cocaine reinstatement of conditioned place preference. Synapse. 2008; 62:886–889. [PubMed: 18792988]
5. Caroni P, Donato F, Muller D. Structural plasticity upon learning: regulation and functions. Nat Rev Neurosci. 2012; 13:478–490. [PubMed: 22714019]
6. Carulli D, Foscarin S, Faralli A, Pajaj E, Rossi F. Modulation of semaphorin3A in perineuronal nets during structural plasticity in the adult cerebellum. Mol Cell Neurosci. 2013; 57:10–22. [PubMed: 23999154]
7. Carulli D, Rhodes KE, Brown DJ, Bonnert TP, Pollack SJ, Oliver K, Strata P, Fawcett JW. Composition of perineuronal nets in the adult rat cerebellum and the cellular origin of their components. J Comp Neurol. 2006; 494:559–577. [PubMed: 16374793]
8. Chaudhri N, Caggiula AR, Donny EC, Booth S, Gharib M, Craven L, Palmatier MI, Liu X, Sved AF. Self-administered and noncontingent nicotine enhance reinforced operant responding in rats: impact of nicotine dose and reinforcement schedule. Psychopharmacology (Berl). 2007; 190:353–362. [PubMed: 16847680]
9. Clemens KJ, Castino MR, Cornish JL, Goodchild AK, Holmes NM. Behavioral and neural substrates of habit formation in rats intravenously self-administering nicotine. Neuropsychopharmacology. 2014; 39:2584–2593. [PubMed: 24823947]
10. Cloke JM, Winters BD. alpha(4)beta(2) Nicotinic receptor stimulation of the GABAergic system within the orbitofrontal cortex ameliorates the severe crossmodal object recognition impairment in ketamine-treated rats: implications for cognitive dysfunction in schizophrenia. Neuropharmacology. 2015; 90:42–52. [PubMed: 25460188]
11. Corrigall WA, Coen KM. Nicotine maintains robust self-administration in rats on a limited-access schedule. Psychopharmacology (Berl). 1989; 99:473–478. [PubMed: 2594913]
12. Corrigall WA, Coen KM, Adamson KL. Self-administered nicotine activates the mesolimbic dopamine system through the ventral tegmental area. Brain Res. 1994; 653:278–284. [PubMed: 7982062]
13. Di Chiara G, Imperato A. Drugs abused by humans preferentially increase synaptic dopamine concentrations in the mesolimbic system of freely moving rats. Proc Natl Acad Sci U S A. 1988; 85:5274–5278. [PubMed: 2899326]
14. Erhardt S, Schwieler L, Engberg G. Excitatory and inhibitory responses of dopamine neurons in the ventral tegmental area to nicotine. Synapse. 2002; 43:227–237. [PubMed: 11835517]
15. Foscarin S, Ponchione D, Pajaj E, Leto K, Gawlak M, Wilczynski GM, Rossi F, Carulli D. Experience-dependent plasticity and modulation of growth regulatory molecules at central synapses. PLoS One. 2011; 6:e16666. [PubMed: 21304956]
16. Ghosheh O, Dwoskin LP, Li WK, Crooks PA. Residence times and half-lives of nicotine metabolites in rat brain after acute peripheral administration of [2′-(14)C]nicotine. Drug Metab Dispos. 1999; 27:1448–1455. [PubMed: 10570026]
17. Gipson CD, Reissner KJ, Kupchik YM, Smith AC, Stankeviciute N, Hensley-Simon ME, Kalivas PW. Reinstatement of nicotine seeking is mediated by glutamatergic plasticity. Proc Natl Acad Sci U S A. 2013; 110:9124–9129. [PubMed: 23671067]
18. Gogolla N, Caroni P, Luthi A, Herry C. Perineuronal nets protect fear memories from erasure. Science. 2009; 325:1258–1261. [PubMed: 19729657]
19. Green TA, Crooks PA, Bardo MT, Dwoskin LP. Contributory role for nornicotine in nicotine neuropharmacology: nornicotine-evoked [3H]dopamine overflow from rat nucleus accumbens slices. Biochem Pharmacol. 2001; 62:1597–1603. [PubMed: 11755112]

20. Green TA, Phillips SB, Crooks PA, Dwoskin LP, Bardo MT. Nornicotine pretreatment decreases intravenous nicotine self-administration in rats. Psychopharmacology (Berl). 2000; 152:289–294. [PubMed: 11105939]
21. Harris AC, Manbeck KE, Schmidt CE, Shelley D. Mecamylamine elicits withdrawal-like signs in rats following a single dose of nicotine. Psychopharmacology (Berl). 2013; 225:291–302. [PubMed: 22868410]
22. Hartig W, Brauer K, Bruckner G. Wisteria floribunda agglutinin-labelled nets surround parvalbumin-containing neurons. Neuroreport. 1992; 3:869–872. [PubMed: 1421090]
23. Kyerematen GA, Morgan ML, Chattopadhyay B, deBethizy JD, Vesell ES. Nicotine metabolism in cigarette smokers and nonsmokers. Clin Pharmacol Ther. 1994; 55:84–87. [PubMed: 8299321]
24. Laviolette SR, van der Kooy D. The motivational valence of nicotine in the rat ventral tegmental area is switched from rewarding to aversive following blockade of the alpha7-subunit-containing nicotinic acetylcholine receptor. Psychopharmacology (Berl). 2003; 166:306–313. [PubMed: 12569428]
25. Lubbers BR, van Mourik Y, Schetters D, Smit AB, De Vries TJ, Spijker S. Prefrontal gamma-aminobutyric acid type A receptor insertion controls cue-induced relapse to nicotine seeking. Biol Psychiatry. 2014; 76:750–758. [PubMed: 24631130]
26. Mansvelder HD, McGehee DS. Cellular and synaptic mechanisms of nicotine addiction. J Neurobiol. 2002; 53:606–617. [PubMed: 12436424]
27. Mazei-Robison MS, Appasani R, Edwards S, Wee S, Taylor SR, Picciotto MR, Koob GF, Nestler EJ. Self-administration of ethanol, cocaine, or nicotine does not decrease the soma size of ventral tegmental area dopamine neurons. PLoS One. 2014; 9:e95962. [PubMed: 24755634]
28. McFarland K, Kalivas PW. The circuitry mediating cocaine-induced reinstatement of drug-seeking behavior. J Neurosci. 2001; 21:8655–8663. [PubMed: 11606653]
29. Murakami T, Murakami T, Su WD, Ohtsuka A, Abe K, Ninomiya Y. Perineuronal nets of proteoglycans in the adult mouse brain are digested by collagenase. Arch Histol Cytol. 1999; 62:199–204. [PubMed: 10399544]
30. Mychasiuk R, Muhammad A, Ilnytskyy S, Kolb B. Persistent gene expression changes in NAc, mPFC, and OFC associated with previous nicotine or amphetamine exposure. Behav Brain Res. 2013; 256:655–661. [PubMed: 24021241]
31. Natarajan R, Harding JW, Wright JW. A role for matrix metalloproteinases in nicotine-induced conditioned place preference and relapse in adolescent female rats. J Exp Neurosci. 2013; 7:1–14. [PubMed: 25157203]
32. Olson VG, Nestler EJ. Topographical organization of GABAergic neurons within the ventral tegmental area of the rat. Synapse. 2007; 61:87–95. [PubMed: 17117419]
33. Pagliusi SR, Tessari M, DeVevey S, Chiamulera C, Pich EM. The reinforcing properties of nicotine are associated with a specific patterning of c-fos expression in the rat brain. Eur J Neurosci. 1996; 8:2247–2256. [PubMed: 8950089]
34. Perry JL, Joseph JE, Jiang Y, Zimmerman RS, Kelly TH, Darna M, Huettl P, Dwoskin LP, Bardo MT. Prefrontal cortex and drug abuse vulnerability: translation to prevention and treatment interventions. Brain Res Rev. 2011; 65:124–149. [PubMed: 20837060]
35. Sanchez V, Moore CF, Brunzell DH, Lynch WJ. Sex differences in the effect of wheel running on subsequent nicotine-seeking in a rat adolescent-onset self-administration model. Psychopharmacology (Berl). 2014; 231:1753–1762. [PubMed: 24271035]
36. Slaker M, Churchill L, Todd RP, Blacktop JM, Zuloaga DG, Raber J, Darling RA, Brown TE, Sorg BA. Removal of perineuronal nets in the medial prefrontal cortex impairs the acquisition and reconsolidation of a cocaine-induced conditioned place preference memory. J Neurosci. 2015; 35:4190–4202. [PubMed: 25762666]
37. Stoker AK, Olivier B, Markou A. Involvement of metabotropic glutamate receptor 5 in brain reward deficits associated with cocaine and nicotine withdrawal and somatic signs of nicotine withdrawal. Psychopharmacology (Berl). 2012; 221:317–327. [PubMed: 22147259]
38. Subramaniyan M, Dani JA. Dopaminergic and cholinergic learning mechanisms in nicotine addiction. Ann N Y Acad Sci. 2015; 1349:46–63. [PubMed: 26301866]

39. Takahashi YK, Roesch MR, Wilson RC, Toreson K, O'Donnell P, Niv Y, Schoenbaum G. Expectancy-related changes in firing of dopamine neurons depend on orbitofrontal cortex. Nat Neurosci. 2011; 14:1590–1597. [PubMed: 22037501]

40. Tolu S, Eddine R, Marti F, David V, Graupner M, Pons S, Baudonnat M, Husson M, Besson M, Reperant C, Zemdegs J, Pages C, Hay YA, Lambolez B, Caboche J, Gutkin B, Gardier AM, Changeux JP, Faure P, Maskos U. Co-activation of VTA DA and GABA neurons mediates nicotine reinforcement. Mol Psychiatry. 2013; 18:382–393. [PubMed: 22751493]

41. Van den Oever MC, Lubbers BR, Goriounova NA, Li KW, Van der Schors RC, Loos M, Riga D, Wiskerke J, Binnekade R, Stegeman M, Schoffelmeer AN, Mansvelder HD, Smit AB, De Vries TJ, Spijker S. Extracellular matrix plasticity and GABAergic inhibition of prefrontal cortex pyramidal cells facilitates relapse to heroin seeking. Neuropsychopharmacology. 2010; 35:2120–2133. [PubMed: 20592718]

42. Vazquez-Sanroman D, Leto K, Cerezo-Garcia M, Carbo-Gas M, Sanchis-Segura C, Carulli D, Rossi F, Miquel M. The cerebellum on cocaine: plasticity and metaplasticity. Addict Biol. 2015; 20:941–955. [PubMed: 25619460]

43. Volkow ND, Fowler JS. Addiction, a disease of compulsion and drive: involvement of the orbitofrontal cortex. Cereb Cortex. 2000; 10:318–325. [PubMed: 10731226]

44. Xue YX, Xue LF, Liu JF, He J, Deng JH, Sun SC, Han HB, Luo YX, Xu LZ, Wu P, Lu L. Depletion of perineuronal nets in the amygdala to enhance the erasure of drug memories. J Neurosci. 2014; 34:6647–6658. [PubMed: 24806690]

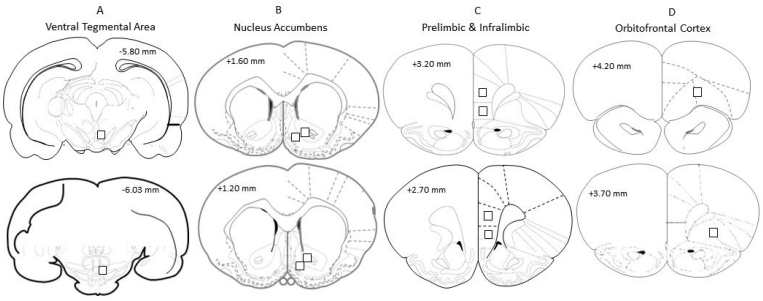

Figure 1.

Schematic representations of coronal stereotaxic sections illustrating the approximate areas for cellular analysis; VTA (Panel A), NAc core and shell (Panel B), PrL and IL portions of mPFC (Panel C) and OFC (Panel D). Black square represents the approximate section where the confocal imaging acquisition occurred. In Panel B, the more lateral square represents the core and the medial square represents the shell; in panel C, the more dorsal square represents the PrL and the ventral square represents the IL.

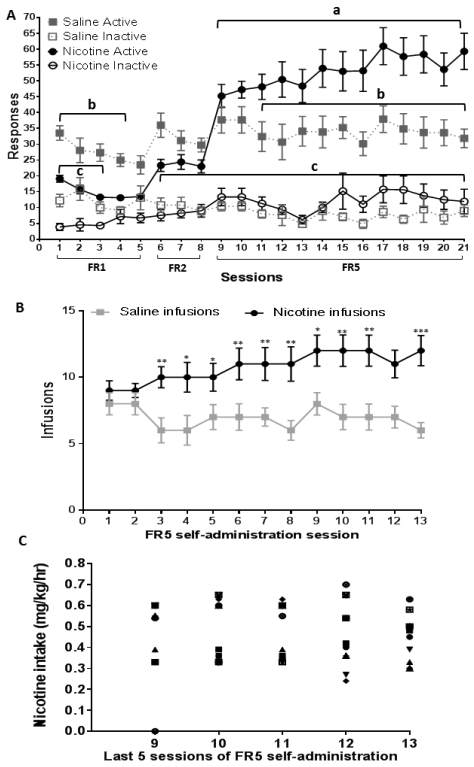

Figure 2.

Behavioral results obtained from nicotine and saline self-administration groups. **A**. Mean (±SEM) number of active and inactive lever responses for saline and nicotine self-administration groups across the 21 acquisition sessions. [a] Represents a within-group difference in active nicotine responses on sessions 9-21 compared to session 1, $p<0.05$. [b] Represents a between-group difference in active responses between saline and nicotine groups, $p<0.05$. [c] Represents a within-group difference in active and inactive responses in the nicotine self-administration group, $p<0.05$. **B**. Mean (±SEM) number of infusions across the FR5 sessions in saline and nicotine self-administration groups; *represents significant difference from saline control, *$p<0.05$, **represents significant difference from saline control, $p< 0.01$. **C**. Nicotine intake per session for individual nicotine self-administration rats, expressed in mg/kg during each of the last five FR5 sessions.

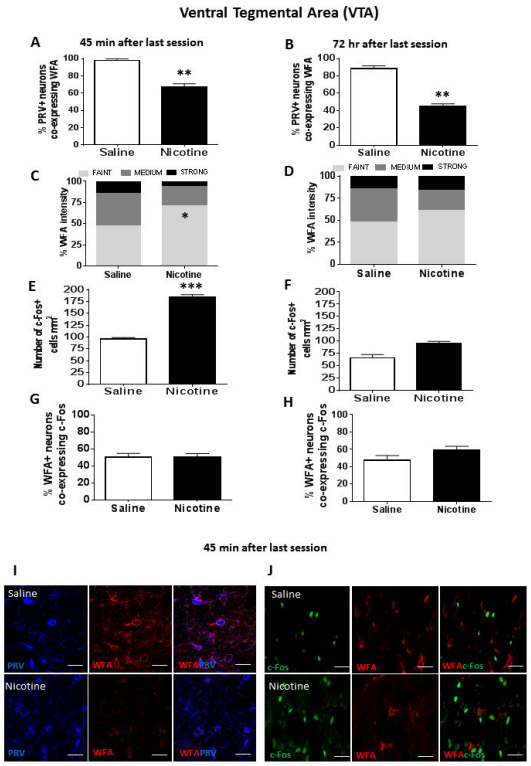

Figure 3.

In top graph panels, immunofluorescence results from VTA showing the percent PRV+ cells co-expressing WFA at either 45 min (Panel A) or 72 hr (Panel B) after the last saline or nicotine self-administration session; **represents significant difference from saline control, $p<0.01$. In second row of graph panels, intensity of WFA+ labelling at either 45 min (Panel C) or 72 hr (Panel D) after the last self-administration session; *represents significant difference in percent faint intensity labelling compared to saline control, $p<0.05$. In third row of graph panels, number of c-Fos+ cells/mm^2 at either 45 min (Panel E) or 72 hr (Panel F) after the last self-administration session; ***represents significant difference from saline control, $p<0.001$. In bottom row of graph panels, percentage of WFA+ cells co-expressing c-Fos at either 45 min (Panel G) or 72 hr (Panel H) after the last self-administration session. Data represent mean +SEM. (I) Confocal images showing representative fluorescent cells in VTA 45 min after the last session. Images show VTA cells expressing PRV or WFA alone, as well as the merge showing co-expression of PRV and WFA. (J) Confocal images showing representative fluorescent cells in VTA 45 min after the last session. Images show VTA cells expressing c-Fos or WFA alone, as well as the merge showing co-expression of c-Fos and WFA. Scale bar represents 20 μm. Images were acquired with a 40x lens with a digital zoom of 2x (80x).

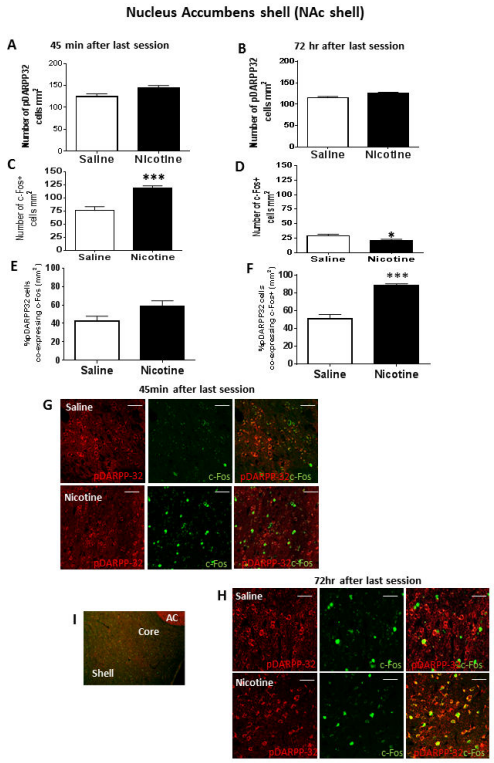

Figure 4.

In the top graph panels, immunofluorescence results from NAc shell showing the number of pDARPP-32 cells per mm^2 at either 45 min (Panel A) or 72 hr (Panel B) after the last session. In the middle row of graph panels, immunofluorescence results showing the number of c-Fos+ cells per mm^2 either 45 min (Panel C) or 72 hr (Panel D) after the last saline or nicotine self-administration session; *represents significant difference from saline control $p<0.05$, ***represents significant difference from saline control $p<0.001$. In the bottom row of graph panels, percentage of pDARRP-32+ cells co-expressing c-Fos at either 45 min (Panel E) or 72 hr (Panel F) after the last session; ***represents significant difference compared to saline control, $p<0.001$. Data represent mean+SEM. (G) Confocal microscope images showing representative fluorescent cells in NAc shell 45 min after the last session. Images show NAc cells expressing pDARPP-32 or c-Fos alone, as well as the merge showing co-expression of pDARPP-32 and c-Fos. (H) Confocal microscope images showing representative fluorescent cells in NAc 72 hr after the last session. Images show NAc cells expressing pDARPP-32 or c-Fos alone, as well as the merge showing co-expression of pDARPP-32 and c-Fos. For panels (G) and (H), scale bar represents 20 μm and images were acquired with a 20x lens with a digital zoom of 2.5x (50x). (I) Representative photoimage showing NAc shell and core subregions relative to anterior commissure (AC).

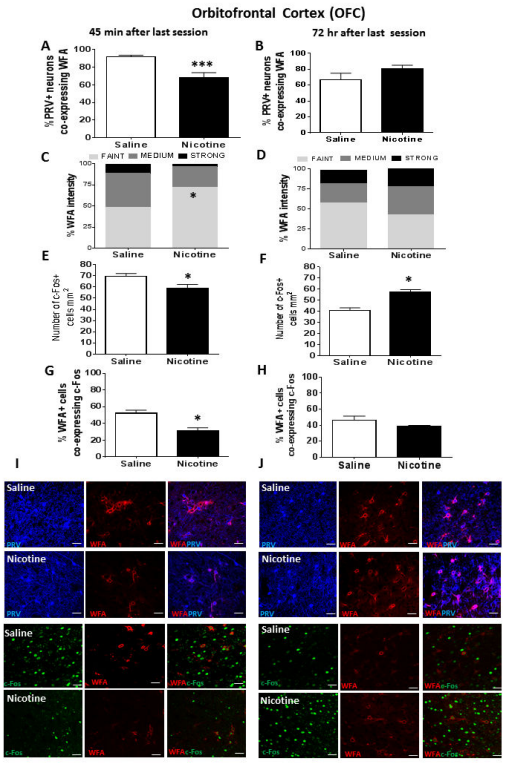

Figure 5.

In the top graph panels, percentage of PRV+ cells in OFC co-expressing WFA at either 45 min (Panel A) or 72 hr (Panel B) after the last self-administration session; ***represents significant difference compared to saline control, $p<0.001$. In the second row of graph panels, intensity of WFA+ labelling at either 45 min (Panel C) or 72 hr (Panel D) after the last self-administration session; *represents significant difference in percent faint intensity labelling compared to saline control, $p<0.05$. In the third row of graph panels, number of c-Fos+ cells/mm^2 at either 45 min (Panel E) or 72 hr (Panel F) after the last self-administration session; *represents significant difference from saline control, $p<0.05$. In the bottom row of graph panels, percentage of WFA+ cells co-expressing c-Fos at either 45 min (Panel G) or 72 hr (Panel H) after the last self-administration session; *represents significant difference from saline control, $p<0.05$. Data represent mean+SEM. (I) Confocal microscopy images showing representative fluorescent cells in OFC 45 min after the last session. First two rows show PRV+ cells and WFA+ cells alone, as well as the merge showing co-expression of PRV and WFA. Bottom two rows show and c-Fos+ and WFA+ cells alone, as well as the merge showing co-expression of WFA and c-Fos. (J) Confocal images showing representative fluorescent cells in OFC 72 hr after the last session. First two rows show PRV+ cells and WFA+ cells alone, as well as the merge showing co-expression of PRV and WFA. Bottom two rows show c-Fos+ and WFA+ cells alone, as well as the merge showing co-expression of c-Fos and WFA. Scale bar represents 20 μm. Images were acquired with a 40x lens with a digital zoom of 2x (80x).

Table 1

Cellular immunofluorescence (# cells per mm^2 or % co-expression) in NAc core, PrL and IL from rats euthanized 45 min or 72 hr after the last saline or nicotine self-administration session. Values represent mean ± SEM. N=6-8 rats per group.

NAc core	**45 min**		**72 hr**	
	Saline	**Nicotine**	**Saline**	**Nicotine**
# c-Fos+ cells	44.6 ± 5.1	**58.1 ± 4.2***	25.7 ± 3.7	26 ± 2.3
# pDARPP32+ cells	105.8 ± 8.5	115.9 ± 6.9	95.3 ± 0.6	96.9 ± 4.2
% pDARPP32+ cells co-expressing c-Fos	45.1 ± 0.9	51.9 ± 1.9	55.3 ± 2.8	52.9 ± 1.7
PrL	**45 min**		**72 hr**	
	Saline	**Nicotine**	**Saline**	**Nicotine**
# PRV+ cells	20.1 ±1.9	19.8 ±0.7	11.8 ± 1.5	15.5 ± 0.8
# WFA+ cells	8.7 ±0.9	7.0 ±0.6	7.1 ± 0.7	10.1 ± 0.6
# c-Fos+ cells	37.5 ± 3.5	34.5 ±3.5	24.5 ± 1.9	28.0 ± 1.5
% PRV+ cells co-expressing WFA	74.0 ±3.1	71.7 ±5.9	63.7 ± 7.5	65.9 ± 10.1
% PRV+ cells co-expressing c-Fos	39.7 ±6.6	34.5 ±4.7	50.0 ± 7.3	55.7 ± 2.2
% WFA+ cells co-expressing c-Fos	45.9 ±8.5	46.8 ±8.3	29.8 ± 3.1	36.1 ± 1.7
IL	**45 min**		**72 hr**	
	Saline	**Nicotine**	**Saline**	**Nicotine**
# PRV+ cells	22.8 ±0.7	21.2 ±0.9	13.0 ± 1.0	15.1 ± 1.4
# WFA+ cells	10.2 ±0.8	10.6 ±1.2	9.3 ± 1.3	10.3 ± 0.8
# c-Fos+ cells	33.7 ±2.0	37.3 ±3.0	20.8 ± 1.7	27.6 ± 1.4
% PRV+ cells co-expressing WFA	69.8 ±4.3	67.2 ±4.5	72.2 ± 8.8	70.5 ± 10.3
% PRV+ cells co-expressing c-Fos	37.6 ±4.3	30.7 ±4.8	64.6 ± 7.5	56.4 ± 6.9
% WFA+ cells co-expressing c-Fos	41.3 ±3.0	30.2 ± 6.5	45.9 ± 6.2	38.2 ± 4.0

* $p<0.05$ compared to saline control.